Earth and Planetary Science Letters 374 (2013) 111–120

Contents lists available at SciVerse ScienceDirect

Earth and Planetary Science Letters

journal homepage: www.elsevier.com/locate/epsl

Brine-assisted anatexis: Experimental melting in the system haplogranite–H_2O–NaCl–KCl at deep-crustal conditions

L.Y. Aranovich [a,b], R.C. Newton [c], C.E. Manning [c,*]

[a] Institute of Geology of Ore Deposits, Petrography, Mineralogy and Geochemistry, Russian Academy of Sciences, Moscow, Russia
[b] Department of Geology, University of Johannesburg, Johannesburg, South Africa
[c] Department of Earth and Space Sciences, University of California, Los Angeles, CA, USA

ARTICLE INFO

Article history:
Received 30 November 2012
Received in revised form
10 May 2013
Accepted 17 May 2013
Editor: T. Elliot
Available online 13 June 2013

Keywords:
granites
anatexis
crustal fluids

ABSTRACT

The first-melting temperature of haplogranite in the presence of H_2O–NaCl–KCl solutions was determined experimentally at deep-crustal conditions of 6–14 kbar and 700–900 °C. Minimum melting occurs at fluid K/(K+Na) of 0.2–0.25. Melting temperature rises strongly with increasing salinity: at 10 kbar, first melting occurs at 800 °C with a H_2O mole fraction (X_{H_2O}) of 0.62 ± 0.02, similar to the salinity of fluid inclusions in minerals of some granites and migmatites. At 900 °C and 10 kbar, X_{H_2O} is 0.33 ± 0.01 for first melting. All minimum melts are granitic over the entire P–T–X_{H_2O} range, with SiO_2 melt concentrations of 74 ± 2 wt% on a H_2O-free basis and Al_2O_3 and alkalis typical for granites. Normative quartz is near 30% for all liquids. The K/(K+Na) ratios of minimum melts increase strongly with decreasing H_2O activity: at 10 kbar and $X_{H_2O} = 1$, K/(K+Na) in the melt is 0.25, whereas at $X_{H_2O} = 0.34$ it is 0.55. This "brine trend" is similar to, but more pronounced than, the trend described by decreasing H_2O activity in H_2O–CO_2 fluids, and it better explains the compositions of K-rich granites. Minimum-melting curves in the presence of brines of constant X_{H_2O} have strongly positive dP/dT slopes at $P > 2$ kbar, in contrast to vertical or negative dP/dT slopes for those in the presence of H_2O–CO_2 fluid. There is therefore a wide P–T range over which migrating low-H_2O-activity brines may generate subsolidus, deep-crustal metasomatism in the form of K_2O and silica enrichment. Moreover, once melting occurs, rising accumulations of granitic magma may be fluid saturated and even increase their melting capacity with decreasing depth because of the strong pressure dependence of H_2O activity in salt solutions. Our results offer an explanation for mid-crust migmatization and granite production: rising hot brines may provoke rock melting at some threshold of decreasing depth in the range 15–20 km. Because of their enhanced capacity for metasomatism, leading to eventual melting at granulite facies conditions of temperature, pressure and H_2O activity, concentrated brines should be considered as possibly important agents in crustal evolution.

1. Introduction

1.1. Saline fluids in granites and migmatites

Fluid inclusion studies of minerals in granites have revealed a surprising new aspect of fluid action in the formation of some granites that may bear on the enigmatic role of H_2O: a possibly important role of concentrated brines. Highly saline fluids in minerals of shallow plutons associated with economic mineral deposits have been described many times since the pioneering work of Roedder (1971). Subsequent studies have shown, moreover, that saline fluid inclusions are not confined to high-level ore-forming granites, but may be more general. Hypersaline fluid inclusions have been reported from the alkaline granites of the Oslo Rift (Hansteen and Burke, 1990), the Archean Closepet Granite of southern India (Srikantappa and Malathi, 2008), plutonic xenoliths from Ascension Island (Harris, 1986), and the Lower Paleozoic Pampleanas granites of Argentina (Lira et al., 2007). Concentrated saline inclusions have also been described in various migmatite complexes (Höller and Hoinkes, 1996; Misiti et al., 2005; Rubatto et al., 2009; Smit and Van Reenen, 1997; Srikantappa and Zargar, 2009; Touret and Olsen, 1985). A study of the southern Closepet K-rich granite (Slaby et al., 2012) revealed complex chemical zoning of K-feldspar megacrysts attributed to the passage of "halogen-rich" solutions of deep-seated origin at magmatic temperatures.

1.2. Water problem in crustal melting

The source of H_2O in the production of granitic magmas is the subject of continuing debate. The model most often discussed is that of fluid-absent melting of mid-to-deep crust rocks of

* Corresponding author. Tel.: +1 3102063290.
E-mail address: manning@ess.ucla.edu (C.E. Manning).

0012-821X/$ - see front matter © 2013 Elsevier B.V. All rights reserved.
http://dx.doi.org/10.1016/j.epsl.2013.05.027

intermediate composition where the major source of H_2O is that of resident micas and amphiboles (Brown, 2001; Stevens et al., 1997; Thompson, 2001). Experimental melting studies have shown that only quite small amounts of granitic liquid can be obtained by "dehydration melting" at temperatures lower than about 900 °C (Johannes and Holtz, 1991). To some workers, this mechanism is insufficient to produce the massive swarms of continent-interior or "A-type" granites like those of Transbaikalia (Litvinovsky and Podladchikov, 1993); major input of H_2O, and probably alkalis and trace elements, must be accomplished by some mechanism. A variety of field and chemical studies have proposed "fluid-assisted" anatexis (Berger et al., 2008; Castro et al., 2003; Cherneva and Georgieva, 2007; Höller and Hoinkes, 1996; Jung et al., 1999; Kalsbeek et al., 2001; Prince et al., 2001; Rubatto et al., 2009; Slagstad et al., 2005).

It is hard to explain, with either the fluid-present or fluid-absent hypotheses, large-scale melting in terranes in which H_2O activity is inferred to have been low, as in the granulite facies diatexite migmatites, with up to 50 vol% of supposed former melt (Friend, 1983; Percival, 1991; Timmermann et al., 2002). Some of these occurrences are in transitional amphibolite facies to granulite facies terranes where the maximum temperatures reached must have been much lower than the ≥900 °C required for large percentage dehydration melting.

1.3. Possible role of brine-induced anatexis

Aranovich and Newton (1996) found in their experimental study of the thermodynamics of the H_2O–NaCl system at high temperatures and pressures that H_2O activity in these fluids becomes quite low at pressures greater than about 4 kbar. They attributed this effect to pressure-induced ionization of solute NaCl. Foreseeable consequences of low H_2O activity in brine pore fluids in deep crustal environments are suppression of hydrous minerals and, at the same time, elevation of the fluid-saturated solidus temperature. In particular, Aranovich and Newton (1996) envisioned the possibility of partial melting of crustal gneisses of intermediate composition in the presence of saline solutions where the granitic liquids formed can coexist with anhydrous minerals of the granulite facies, the pyroxenes and garnets. In this postulated brine-assisted anatexis, there would be no theoretical limit to the amount of H_2O available for melting as long as brine infiltration persists.

The present study of the melting of granite in the simple system $KAlSi_3O_8$ (Or)–$NaAlSi_3O_8$ (Ab)–SiO_2 (Qz) in the presence of NaCl–KCl–H_2O solutions at deep-crustal pressures (6–14 kbar) and temperatures (700–900 °C) was undertaken to quantify the conditions at which brine-saturated granitic magmas may exist in the Earth's crust.

2. Experimental methods

Starting materials were synthetic and natural K-feldspar (microcline), natural albite and natural quartz. The largest detectable impurities in the natural feldspars were <0.1 wt% Na_2O in the microcline and <0.1 wt% CaO in the albite. A finely ground mixture of the minerals was prepared on the composition $Or_{30}Ab_{40}Qz_{30}$ (wt%), simulating the composition of natural leucogranite. This mix was homogenized by repeated grinding under acetone in an agate mortar.

Weighed quantities of the mix were sealed in Pt tube segments of 2.5 or 3.5 mm diameter with H_2O–NaCl–KCl solutions of various mole fractions of H_2O ($X_{H_2O} = n_{H_2O}/(n_{H_2O} + n_{NaCl} + n_{KCl})$, where n is moles) from 0.3 to 0.9. The larger diameter tubing was used to accommodate the considerable amounts of salt in the low-H_2O runs. The weight of H_2O was chosen so that the alkali content of the fluid would be large compared to that of the melt or the feldspar (generally by a factor of 5–42; Table 1). The fluids were therefore effectively buffered against exchange with the condensed phases. Ingredient weighing order was silicate mix, KCl, NaCl, and H_2O. We achieved target solution compositions by adding a small excess of H_2O and allowing it to evaporate on the balance until the desired weight was achieved. All weighing was carried out using a Mettler M3 microbalance ($1\sigma = 2$ μg).

The fluid–rock ratio in the experiments averaged 4.7 (Table 1), which should nominally preclude significant shift in fluid composition. Therefore an essential first step was to determine the appropriate K/Na range in the fluid at which to determine minimum melting conditions. Experimental alkali exchange between (Na, K) chloride solutions and (Na, K) feldspars at lower pressures and temperatures and more dilute concentrations (Iiyama, 1965; Orville, 1963) indicate that the molar K–Na ratio ($K^{fl} = n_K/(n_{Na}+n_K)$) in the solutions is in the range 0.2–0.3 in equilibrium with both sanidine and albite. We carried out a preliminary series of experiments at 900 °C, 10 kbar, $X_{H_2O} = 0.4$, and a range of K^{fl}, to examine alkali exchange between synthetic high structural state feldspars and fluids. Starting materials were synthetic high albite, synthetic sanidine, and synthetic high-structural state intermediate feldspars. Compositions of exchanged feldspars were determined by X-ray diffraction using methods in Goldsmith and Newton (1974). The results indicated that K^{fl} for minimum melting lies in the range 0.2–0.3. This was confirmed by

Table 1
Summary of experimental results.

Run	P (kbar)	T (°C)	Time (h)	m_{fl}/m_r	alk_{fl}/alk_r	K^{fl}	X_{H_2O}	Run products
25	6	700	97	2.09	5.0	0.201	0.817	Qtz+Fsp
30	6	700	93	0.84	1.7	0.199	0.856	Gl+Qtz+Fsp
18	6	800	48	3.67	19.8	0.199	0.504	Qtz+Fsp
19	6	800	46	7.70	38.0	0.300	0.351	Qtz+Fsp
21	6	800	44	2.87	15.4	0.197	0.542	Gl+Qtz+Fsp
16	6	800	46	2.36	7.7	0.200	0.701	Gl
34	6	850	47	6.72	32.7	0.200	0.308	Qtz+Fsp
38	6	850	43	7.17	34.1	0.200	0.353	Gl+Qtz+Fsp
47	6	850	73	8.69	42.6	0.250	0.329	Qtz+Fsp
9	10	800	43	3.83	14.7	0.199	0.601	Qtz+Fsp
15	10	800	47	3.16	11.5	0.199	0.634	Gl
13	10	800	46	2.39	7.7	0.192	0.706	Gl
14	10	800	46	1.83	4.5	0.219	0.810	Gl
3	10	870	42	6.37	28.1	0.201	0.461	Gl
6	10	900	47	7.26	35.0	0.201	0.324	Qtz+Fsp
7	10	900	48	6.07	28.9	0.201	0.348	Gl+Qtz+Fsp
5	10	900	48	4.61	21.8	0.198	0.361	Gl
2	10	900	70	3.99	17.5	0.201	0.463	Gl
40	10	900	50	5.87	25.7	0.200	0.469	Gl
10	10	900	40	3.02	13.2	0.209	0.609	Gl
11	10	900	40	2.37	12.5	0.200	0.688	Gl
43	10	900	50	6.02	29.3	0.250	0.344	Gl+Qtz+Fsp
12	10	900	63	7.65	43.3	0.300	0.314	Qtz+Fsp
20	10	900	72	7.23	35.7	0.299	0.350	Gl+Qtz+Fsp
8	10	900	29	6.93	33.7	0.300	0.375	Gl+Qtz+Fsp
39	10	900	46	3.43	15.7	0.499	0.595	Gl
37	10	900	47	3.83	14.7	0.698	0.602	Gl
33	14	750	66	2.65	8.6	0.199	0.701	Qtz+Fsp
36	14	750	67	2.22	6.7	0.198	0.740	Gl+Qtz+Fsp
24	14	750	51	2.11	5.9	0.197	0.768	Gl
28	14	900	18	6.65	30.6	0.200	0.402	Qtz+Fsp
22	14	900	23	5.50	24.5	0.199	0.444	Gl+Qtz+Fsp
50	14	900	68	5.96	27.6	0.250	0.421	Gl+Qz+Fsp

Explanation: m_{fl}/m_r is the initial mass ratio of fluid components (H_2O+NaCl+KCl) to crystals ("rock") added to an experiment; alk_{fl}/alk_r is the initial molar ratio of Na+K in the fluid to that in the crystals ("rock") in an experiment; K^{fl} is the molar K–Na ratio, $n_K/(n_{Na}+n_K)$, in the fluid phase; X_{H_2O} is the H_2O mole fraction in the fluid, $n_{H_2O}/(n_{H_2O} + n_{NaCl} + n_{KCl})$.

additional experiments during the course of this study (see below). Accordingly, our definitive solidus determinations used alkali ratios in this range.

All solidus determinations and fluid–melt equilibrations were performed in the 2.54-cm diameter piston-cylinder apparatus with NaCl pressure medium and graphite heater sleeves. Temperatures were controlled automatically using Pt vs. Pt 10% Rh (Type S) thermocouples. Pressure uncertainties were ± 30 MPa and temperature uncertainties were ± 3 °C. The great advantage of this technique is the rapid quench rate possible (to below 200 °C in 12 s).

Quenched capsules were cleaned and weighed to verify that there was no fluid escape during the runs. The capsules were then punctured with a needle, dried for 2 h at 115 °C, and reweighed to check the H_2O mole fraction of the fluid. Salt was leached from the quenched charges using distilled H_2O. The charges were characterized by polarizing microscope, X-ray diffraction, scanning electron microscope (SEM) and electron microprobe. Electron microprobe analysis conditions were 15 keV operating voltage and 15 nA beam current. The spot size was 15 μm for glasses and 5 μm for feldspar crystals. Constancy of alkali element counts from glasses over 20 s indicated no detectable alkali loss. For a number of glasses oxygen was quantitatively analyzed as an unknown using natural albite as a standard for O; the totals of cations plus oxygen were near 100% in those analyses, if appropriate amounts of hydrogen (0.5–1.5 wt%) were added.

3. Results

3.1. Detection of melting

Experimental conditions and results are given in Table 1. Melting could be detected unambiguously by inspection of quenched charges under the binocular microscope (Fig. 1A). Investigation of portions of the charges using immersion-oil mounts and a polarizing microscope confirmed the interpretations and allowed identification of crystalline phases. Quenched silicate melt was evident in the form of numerous clear glass spheres (Fig. 1A and B), often accompanied by a large milky-white glass bead in completely melted charges. Some of the near-solidus charges contained doubly terminated quartz crystals and aggregates of small equant feldspars, as well as glass beads or spheres (Fig. 1C). Polished mounts of selected glass beads showed numerous fluid inclusions of ~20 μm diameter with salt daughter crystals.

3.2. Feldspar and glass compositions

Feldspar compositions as determined by microprobe analysis are given in Supplementary Data Table S1. No differences in feldspar composition could be determined between feldspar aggregates grown in the fluid and phenocrysts occurring in the quenched glass. The 800 °C runs showed equilibrated rims of intermediate feldspar on unequilibrated residual albite crystals (Fig. 1D), whereas feldspar in runs at higher temperature display no such zoning. Compositions of feldspar coexisting with glass in <800 °C experiments showed variable compositions, probably indicative of subsolvus conditions. As a whole, the results were consistent with the *P–T* trace of the alkali feldspar solvus crest (Brown and Parsons, 1981).

Glass compositions of near-solidus charges are granitic, ranging from 72 to 76 wt% SiO_2 when restored to a 100% oxide basis (Supplementary Data Table S2). K/Na ratios are always higher than in the equilibrium fluid phase and depend strongly on that ratio. Chlorine contents of the liquids are small, ranging from 0.17 to 0.71 wt%. All glasses yield oxide totals less than 100 wt%, consistent with the presence of dissolved H_2O. The quenched glasses in which microprobe totals indicated H_2O contents in the range 7–10 wt% showed myriad dusty inclusions, undoubtedly exsolved sub-micron vesicles, which impart a slight brown color to glass fragments in immersion oils. Glasses showing >10 wt% H_2O contained abundant bubbles. The low microprobe totals result from a combination of H_2O still dissolved in the glass and uniformly distributed empty or filled microvesicles. The inferred H_2O contents of high-H_2O glasses are therefore probably lower limits.

3.3. Fluid composition at the melting minimum

To check the assumption about the alkali ratio in the fluid at which to conduct the experiments, we supplemented the preliminary experiments at 900 °C, 10 kbar, with additional runs over a wide range of X_{H_2O}, in which feldspar and glass compositions were determined by electron microprobe analysis (Fig. 2). All of the quenched near-solidus charges, including those with glass, contained quartz and a single alkali feldspar, consistent with *T* greater than closure of the alkali feldspar solvus (e.g., Brown and Parsons, 1981). Electron microprobe analysis of these feldspars demonstrates that the fluid-feldspar alkali distribution agrees with those from the exchange experiments, in which feldspar composition was determined by X-ray diffraction (Fig. 2). Compositions of coexisting glasses identify K^{fl} at minimum melting, where $K/(K+Na)_{glass}=K/(K+Na)_{feldspar}$. This is the same approach used to determine the minimum melt composition in the haplogranite–H_2O and haplogranite–H_2O–CO_2 systems (Ebadi and Johannes, 1991; Luth et al., 1964; Tuttle and Bowen, 1958). Fig. 2 illustrates that compositions of supersolvus feldspar that coexisted with fluid and melt are poorer in K than the melt at $K^{fl}=0.2$, but richer in K for fluids of $K^{fl}=0.3$. The melt and feldspar are inferred to have the same K/(K+Na) at $K^{fl}=0.24$, though uncertainties are sufficiently large that we can be confident only that the supersolvus invariant melting minimum lies somewhere in the range $K^{fl}=0.2$–0.3. Nevertheless, this is consistent with results at lower pressure (Iiyama, 1965; Orville, 1963). All minimum melt determinations were therefore made at $K^{fl}=0.2$–0.25.

Successful experiments require that K^{fl} does not change during runs. That this condition was realized was confirmed by post-run analysis of several quenched salt samples, which were dissolved in H_2O and analyzed by ion chromatography.

3.4. Invariant minimum melting

The first melting points encountered at each temperature and pressure as H_2O in the fluid increased correspond to those of an invariant minimum, as shown by the small H_2O mole fraction over which crystals and glass were found together in the quenched charges. At 800 °C and 10 kbar the quenched charge was entirely crystalline at $X_{H_2O}=0.601$ and entirely glass at $X_{H_2O}=0.634$. That the first melting temperature is not greatly sensitive to change of K^{fl} of the fluid in the range $0.2\leq K^{fl}\leq 0.3$ is shown by the fact that the H_2O contents of the solidus fluids at 800 and 900 °C, 10 kbar, were indistinguishable in this range and that runs at $K^{fl}=0.25$ within the brackets defining the solvus at $K^{fl}=0.2$ and 0.3 showed the assemblage glass+feldspar+quartz. The small mole fraction intervals over which melting occurred at a given *P* and *T*, the homogeneity of the feldspars at ≥800 °C, and the consistency of the isobaric T–X_{H_2O} melting curves with the corresponding melting points in the pure-H_2O system (Huang and Wyllie, 1975; Luth et al., 1964) all give evidence that the present minimum melting determinations reflect close approach to chemical equilibrium.

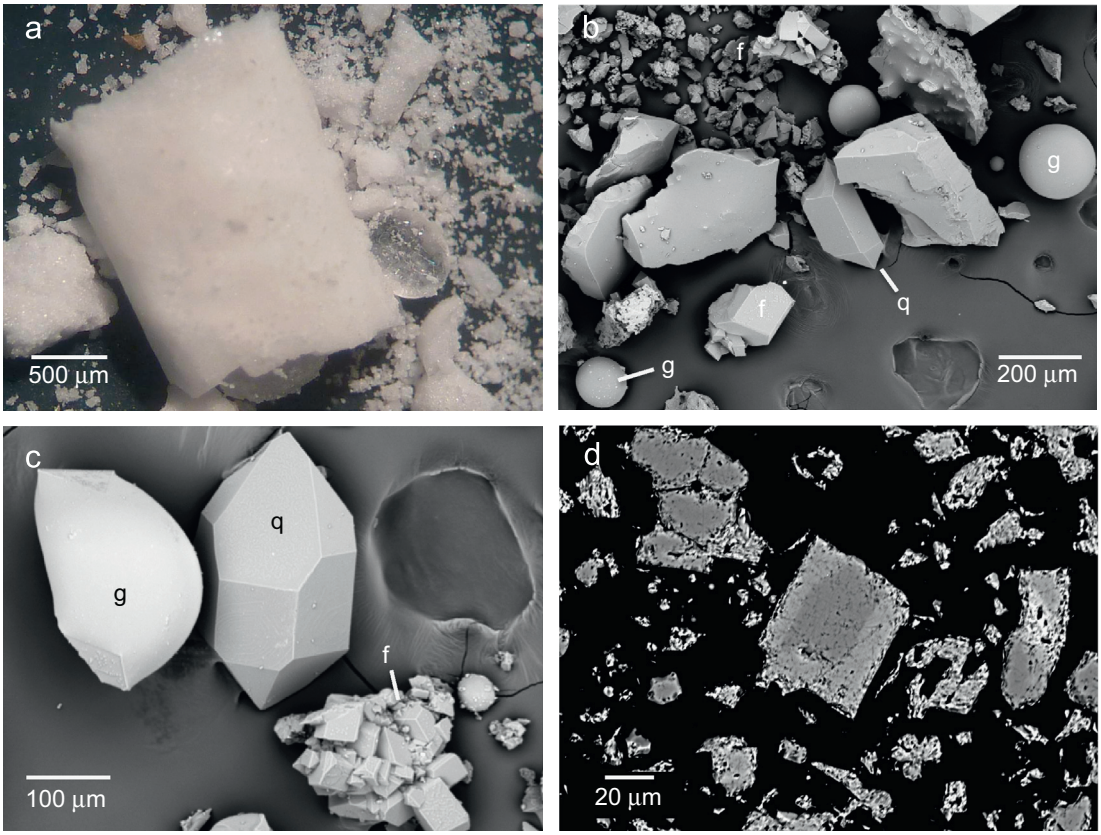

Fig. 1. Images of run products. *Abbreviations:* g, glass; q, quartz; f, feldspar. (A) Plain-light image of quenched and dried charge, showing salt cake largely preserving capsule dimensions, and a large, translucent, glass spheroid indicating presence of melt during the experiment (Run 3, 10 kbar, 870 °C, Table 1). (B) and (C) Secondary electron photomicrograph of portions of Run 20 products (10 kbar, 900 °C, Table 1) with salt removed by dissolution in H_2O. Glass spheres and chunks, quartz crystals, and aggregates of smaller feldspar crystals present. (D) Backscattered electron photomicrograph of recrystallized feldspars from Run 18 (6 kbar, 800 °C, Table 1). The grain in the center of field of view displays equilibrated feldspar of composition Or 24 which overgrew a starting albite crystal.

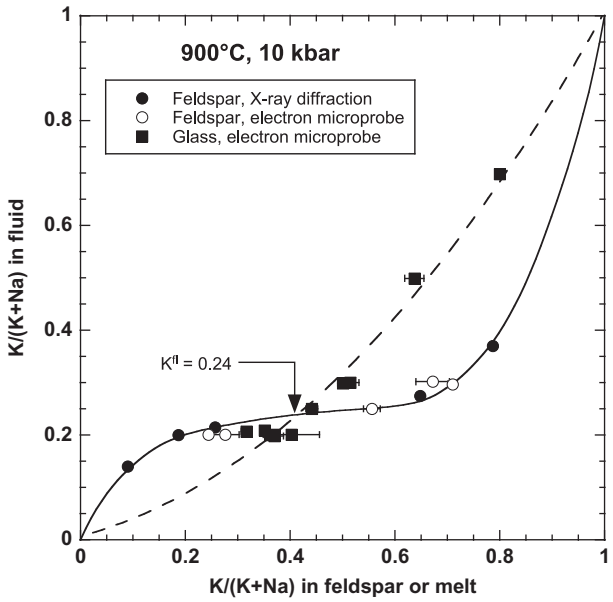

Fig. 2. Alkali element compositions of coexisting feldspars and melts versus the alkali composition of the coexisting chloride fluids at 900 °C and 10 kbar. Feldspar compositions determined by X-ray diffraction (filled circles) and by electron microprobe (open circles, Supplementary Data Table S1) agree well. The trend of feldspar composition (solid line) with liquid composition (filled squares, dashed line) intersect at the minimum melting point, corresponding to $X_K = K/(K+Na)$ (K^{fl}) of 0.24. However, the X_{H_2O} of the melting point was quite insensitive to X_K in the range 0.2–0.3 (Table 1), even though the feldspar composition changes drastically in this range. The extreme change of the feldspar composition with small change of the fluid composition may have a bearing on the origin of very K-rich granites.

3.5. *Solidus as a function of P, T, and X_{H_2O}*

Experimental brackets defining the solidus temperatures at 6, 10 and 14 kbar are shown in Fig. 3. It is evident that the salt component of the aqueous fluid greatly elevates the temperatures of haplogranite solidus minima above pure H_2O values, and that the effect increases with pressure. At 10 kbar, the simple granite melting minimum is 125 °C higher with 30 mol% salt than in pure H_2O.

4. Discussion

4.1. *Minimum melts in the haplogranite–brine system*

4.1.1. *H_2O concentration of melts*

Oxide totals for the 10 kbar glasses (Fig. 4; Supplementary Data Table S2) decrease linearly from ~96 wt% at the solidus to ~88 wt% for the most H_2O-rich fluid composition. Care was taken to minimize Na migration during analysis, so the data provide an estimate of the H_2O contents of the liquids at run conditions. Although errors may be large (e.g., Devine et al., 1995), two observations support this assumption: the sum of the oxygen and cation analyses was close to 100%, and the trend of the probe totals projects to 100% at zero H_2O in the fluid (Fig. 4), which is required for an anhydrous glass.

The H_2O contents of granitic minimum melts as indicated by the microprobe totals are substantially larger than given by models (Johannes, 1985a; Johannes and Holtz, 1991) at the same temperature and pressure. At 900 °C and 10 kbar, Johannes (1985b) gives 3.5 wt % H_2O and Johannes and Holtz (1991) give only 2.3 wt%,

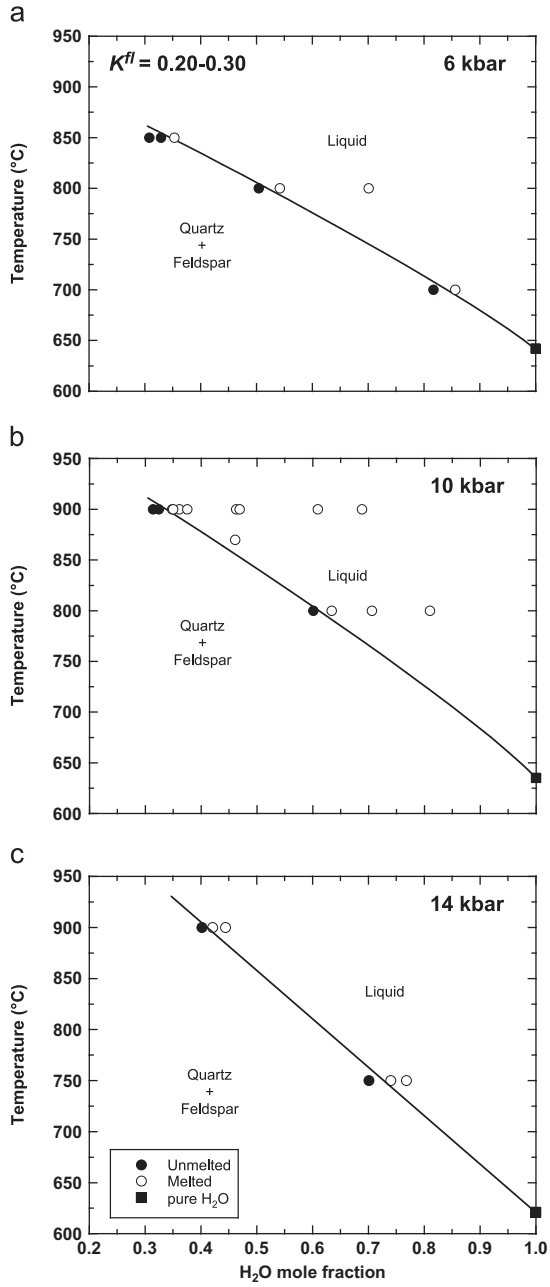

Fig. 3. Minimum melting temperatures of haplogranite as a function of the H_2O mole fraction in coexisting alkali-chloride fluids at 6 (A), 10 (B) and 14 kbar (C). Melting points of simple granite in pure H_2O are compiled from Luth et al. (1964), Huang and Wyllie (1975) and Johannes and Holtz (1996).

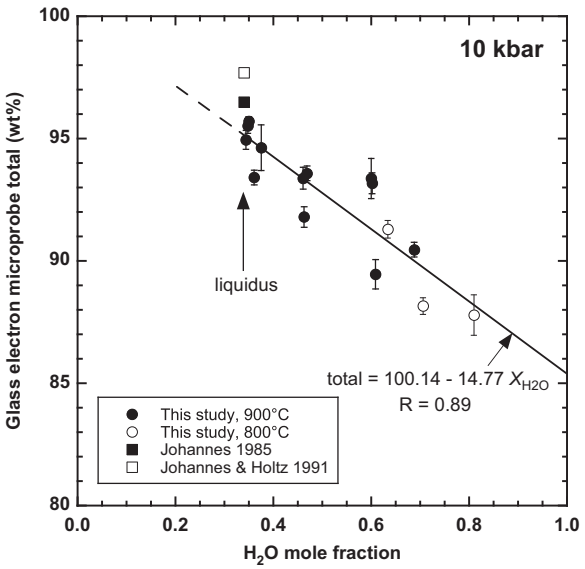

Fig. 4. Oxide totals of electron microprobe analyses of glasses vs. H_2O mole fraction in the coexisting fluid, from 10 kbar experiments (Supplementary Data Table S2). The good correlation and linear extrapolation very close to 100% at zero H_2O mole fraction in the chloride fluids suggest that the totals are indicative of actual H_2O contents of melts at run conditions. Visible microvesicles in some of the glasses suggest that the departures from 100% totals result partly from H_2O still dissolved in the glasses and partly from uniformly distributed microvesicles. Results from this study suggest that H_2O concentration in the minimum melt (solidus) is ~95%, higher than previously inferred by Johannes (1985a) and Johannes and Holtz (1991).

whereas our indication from microprobe totals is close to 5 wt% (Fig. 4). It should be emphasized that the earlier estimates are extrapolations from lower-pressure measured data and do not take into account the close approach at deep-crustal melting conditions to the critical curve in the system albite–H_2O (Shen and Keppler, 1997) or the critical end-point in the system silica–H_2O (Newton and Manning, 2008), under which *P–T* conditions the H_2O contents of undersaturated melts coexisting with crystals must be considerably higher than portrayed by extrapolation from lower pressure data.

4.1.2. Implications for H_2O activity at the solidus

The small Cl contents of the granitic liquids at the solidi (0.17–0.71 wt%, Supplementary Data Table S2) are similar to CO_2 contents at the same conditions in the simple granite–H_2O–CO_2 system (Ebadi and Johannes, 1991). This result implies that melting temperature in the granite–H_2O–CO_2 and granite–brine systems depends solely on the H_2O activity. If true, the Ebadi and Johannes (1991) experimental data in the granite–H_2O–CO_2 system, together with updated H_2O activities in the H_2O–CO_2 system (Aranovich and Newton, 1999), should predict the melting temperatures of a haplogranite in H_2O–NaCl–KCl fluids at the same pressures and H_2O activities. Both Ebadi and Johannes (1991) and this study determined melting at 10 kbar, so we used this pressure to test the hypothesis.

Fig. 5 compares the Ebadi and Johannes (1991) haplogranite solidus in the presence of H_2O–CO_2 to that predicted for H_2O–NaCl–KCl fluids assuming that the melting point is determined uniquely by the H_2O activity at the same temperature, using the H_2O activities in NaCl–KCl brines from Aranovich and Newton (1997). Data from the present study are superimposed on the predicted solidus. The excellent agreement lends strong support to the inference that melting temperature depends almost entirely on H_2O activity alone.

Assuming that this relation holds for the simple granite–brine system over the range of crustal *P* and *T*, we can compute the solidus using the Ebadi and Johannes (1991) data in the H_2O–CO_2 system at 0–10 kbar (their Fig. 8 and 9) and the Aranovich and Newton activity model for H_2O–NaCl–KCl fluids. Results are shown in Fig. 6. It is evident that the minimum-melting temperature at a given pressure and H_2O concentration is much higher in H_2O–NaCl–KCl solutions than in H_2O–CO_2 fluids at pressure greater than about 3 kbar. The pronounced positive dP/dT slopes of X_{H_2O} isopleths in the brine system may have important implications for fluid-assisted anatexis in the deeper crust, as discussed below.

4.1.3. Trends in minimum melt compositions

Table 2 gives CIPW normative compositions for eight near-solidus quenched liquids (glasses) coexisting with quartz and

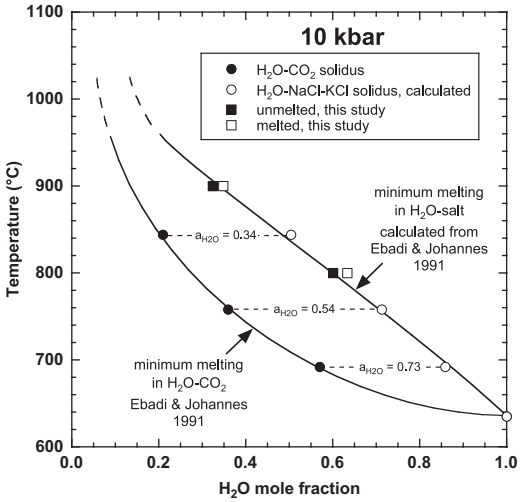

Fig. 5. Comparison of X_{H_2O} of minimum melting for H_2O–CO_2 and H_2O–NaCl–KCl fluids at 10 kbar. Filled circles are data from Ebadi and Johannes (1991) in H_2O–CO_2 fluids. Values of a_{H_2O} were calculated from their X_{H_2O} using the Aranovich and Newton (1999) activity model (note that use of this more precise model slightly changes values of a_{H_2O} reported by Ebadi and Johannes (1991), who used the model of Kerrick and Jacobs (1981)). Corresponding values of X_{H_2O} in H_2O–NaCl–KCl fluids were then calculated at the same a_{H_2O} (Aranovich and Newton, 1997) (short dashed lines), yielding the variation in X_{H_2O} of minimum melting with T in salt solutions predicted using the data Ebadi and Johannes (1991) (open circles). Data from the present study agree well, suggesting that H_2O activity is the primary control on variation in minimum melting. Note that data of Ebadi and Johannes (1991) at low a_{H_2O} and dry conditions are omitted because subsequent work (Holtz et al., 2001) showed them to be inaccurate.

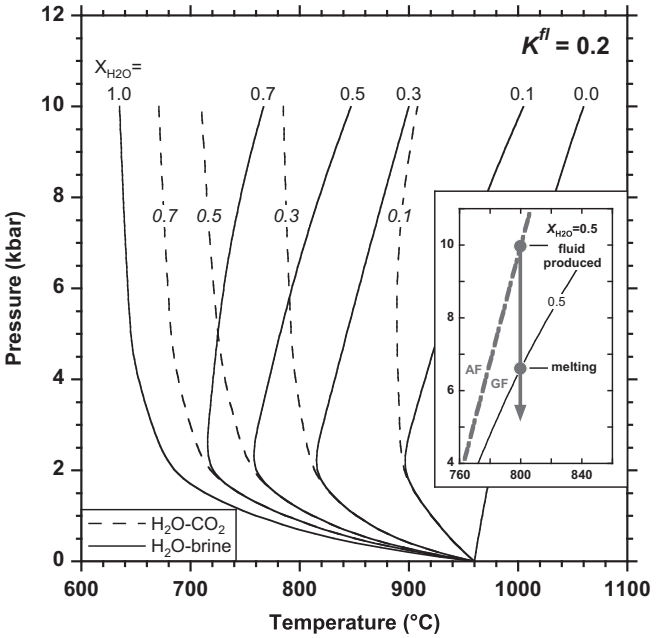

Fig. 6. Isopleths of H_2O mole fraction in the fluid phase in equilibrium with solids and melts at the beginning of haplogranite melting. The dashed curves were derived from the results of Ebadi and Johannes (1991) on melting of a haplogranite in CO_2–H_2O fluids. Values of X_{H_2O} were derived from their reported variation of minimum-melting temperature on X_{H_2O} at 2, 5, and 10 kbar, with minor smoothing. Water activity was calculated using the model of Aranovich and Newton (1999), and then X_{H_2O} in a brine-saturated minimum melt (solid curves) was computed at the same H_2O activity using the Aranovich and Newton (1997) activity model. Calculations assumed $K^{fl}=0.2$, but the isopleths change little for K^{fl} in the range 0.2–0.3 (see text). Inset shows hypothetical brine-induced melting scenario in which a NaCl–KCl solution of $X_{H_2O}=0.5$ is released into the crust at a depth equivalent to 10 kbar during metamorphism. During ~isothermal decompression (bold gray arrow), the fluid does not produce melting until it rises to a shallower level equivalent to ~7 kbar, where it intersects the $X_{H_2O}=0.5$ minimum-melting isopleth. Such a fluid could therefore produce metasomatism at granulite-facies (orthopyroxene-stable) metamorphic conditions in the absence of melting. Dashed bold gray line denotes the approximate boundary between amphibolite facies (AF) and granulite facies (GF), as depicted by Aranovich and Newton (1998).

feldspar. Departures from the Ab–Or–Qz ternary are negligible: minor chlorine was accommodated as normative halite, and compositions are therefore slightly corundum normative.

Fig. 7 shows the normative compositions in the Ab–Or–Qz triangle for 6, 10, and 14 kbar experiments, together with comparable normative compositions of first melts in the haplogranite–H_2O and haplogranite–H_2O–CO_2 systems (Ebadi and Johannes, 1991; Johannes and Holtz, 1996). The present brine-saturated haplogranitic liquids show two significant features that depart from melts coexisting with H_2O and H_2O–CO_2 fluids. In the pure-H_2O system, increasing pressure greatly expands the primary volume of quartz, driving the liquids in equilibrium with quartz and feldspar toward syenitic compositions. Also, the K/(K+Na) ratio of the liquids steadily decreases with pressure, moving the liquids toward granodioritic or trondjhemitic compositions. In the H_2O–CO_2 system, normative quartz remains low at elevated pressure, but the K/(K+Na) advances somewhat with pressure. The granite–brine system shows a different trend, termed here the "brine trend," in which both high normative quartz and high K/(K+Na) ratios are maintained with increasing pressure. The trend indicates that partial melts of intermediate rocks at deep-crustal pressures in the presence of chloride brines will have the compositions of K-rich granites, though the brines may be very Na-rich.

Table 2
Normative compositions of minimum melts.

Run number	P (kbar)	T (°C)	Albite (wt%)	Quartz (wt%)	Kspar (wt%)	Halite (wt%)	Corundum (wt%)	NS (wt%)
30	6	700	35.08	35.09	28.11	0.31	1.36	
21	6	800	29.87	35.13	32.91	0.68	1.31	
38	6	850	28.66	31.24	38.72	0.86	0.40	
15	10	800	41.50	29.90	26.84	0.86	0.79	
7	10	900	41.60	31.59	25.75	0.68	0.29	
20	10	900	31.56	28.56	38.53	0.82		0.42
36	14	750	36.17	30.86	29.23	0.82	2.82	
22	14	900	40.83	27.23	29.74	1.24	0.79	

Abbreviation: NS, Na metasilicate (Na_2SiO_3).

4.2. Petrologic applications

4.2.1. Metasomatism and beginning of melting in the deep crust

The most important results of the present study are the great increase of first-melting temperature of a leucogranite in the presence of an alkali-chloride brine over that in pure H_2O or in H_2O–CO_2 solutions of equivalent H_2O mole fractions, and the distinct brine trend described by minimum melt compositions as H_2O activity declines. The large increase in melting temperature (Fig. 6) results from the great decrease with increasing pressure of H_2O activity in alkali chloride solutions, as reported by Aranovich and Newton (1996, 1997). The low-H_2O-activity saline fluids are nevertheless chemically very reactive in rock systems: they have much higher solubilities for silicate minerals than CO_2–H_2O fluids of the same H_2O concentrations (Newton and Manning, 2000, 2002, 2006, 2007, 2010; Shmulovich et al., 2001), and high solubility for accessory minerals including the phosphates apatite and monazite (Antignano and Manning, 2008; Tropper et al., 2011), which are important carriers of radioactive and rare earth elements. There is thus a large P–T window for high-grade metasomatism available with concentrated brines for sub-solidus alteration of the deep crust by aqueous solutions. The possibilities

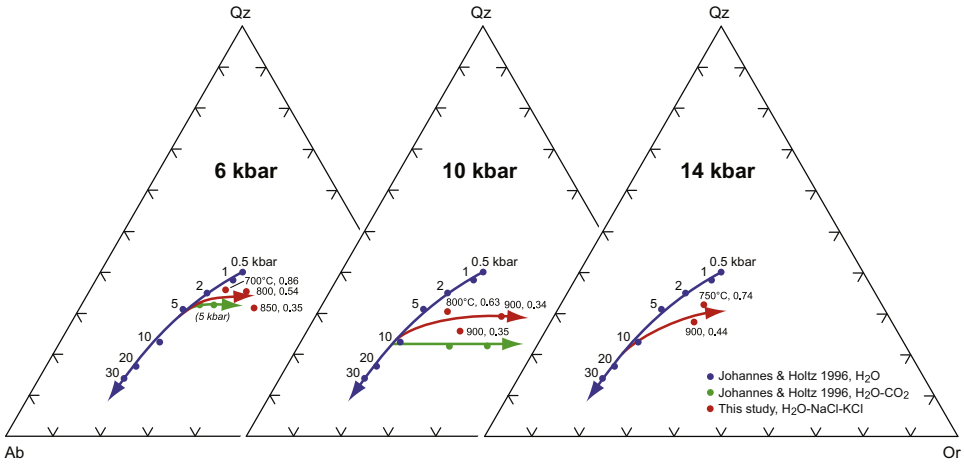

Fig. 7. Quartz–albite–orthoclase ternaries comparing data from this study to previous results, at 6, 10, and 14 kbar. Blue circles show normative compositions of H_2O-saturated minimum melts at a range of compositions (Johannes and Holtz, 1996) and illustrate the trend to SiO_2-poor compositions with rising pressure. Green circles show that isobaric shifts in first melts with rising CO_2 concentration (Ebadi and Johannes, 1991) yield progressively more K-rich melts at constant normative quartz. In contrast, melting in the presence of H_2O–brine yields a distinct brine trend, in which minimum melts become enriched in both normative quartz and orthoclase with increasing salt concentration. Note that 5 kbar H_2O–CO_2 data (Ebadi and Johannes, 1991) are compared to 6 kbar brine data. (For interpretation of the references to color in this figure legend, the reader is referred to the web version of this article.)

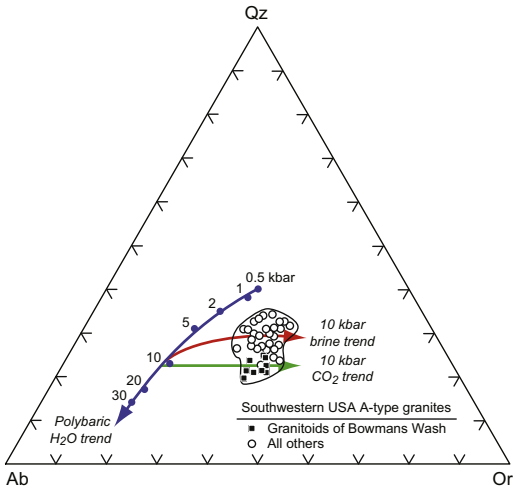

Fig. 8. Quartz–albite–orthoclase ternary comparing trends in normative minimum melt compositions from experiments with compositions of southwestern USA A-type granites (Anderson and Bender, 1989).

for alkali exchange and transport are large, even at granulite-facies conditions of low H_2O activity. Addition of K_2O and SiO_2 by such fluids in intermediate gneisses of the deep crust could move the rocks toward more easily melted compositions.

The distinct brine trend described by minimum melt compositions as salt concentration increases in the coexisting fluid may have fundamental implications for the origin of K-rich granite suites. Fig. 8 illustrates the principal composition range of K-rich, A-type granites from the southwestern USA from Anderson and Bender (1989) (compositions affected by feldspar accumulation are neglected). Anderson and Bender (1989) suggest that these compositions are consistent with minimum melts when the Ca content of plagioclase is taken into account; however, this assumes melting in the presence of pure H_2O. Such melting would produce very high H_2O concentrations, inconsistent with the characteristically low H_2O contents of A-type granites (Anderson and Bender, 1989). The granite compositions more likely reflect melting at reduced H_2O activity. Assuming melting at $\sim$10 kbar, normative Qz–Ab–Or compositions of 21 of 22 investigated granite bodies are too quartz-rich to be consistent with H_2O–CO_2 fluids (the exception is granitoids from Bowmans Wash, California). However, melting in the presence of an H_2O–salt solution could produce the observed compositions. The illustrative granite suite has compositions consistent with K-rich granites elsewhere, some of which possess other geochemical and petrological characteristics suggestive of melting in the presence of a saline fluid (e.g., Harris and Marriner, 1980).

4.2.2. *K–Na partitioning between fluid and feldspar*

Fig. 2 shows the extreme dependence of feldspar Or content with change in K^{fl} of the coexisting brine at 900 °C and 10 kbar. Even though the *P–T* conditions are considerably supersolvus in the alkali feldspar system (Parsons, 1978; Yund and Tullis, 1983), the behavior is similar to sub-solidus feldspar–brine equilibrium at lower *P–T* conditions. Thus, very K-rich alkali feldspars can coexist with Na-rich brines and only moderately K-enriched granite melts. Slight shifts in fluid K/(K+Na) result in large changes in feldspar composition, as emphasized by Orville (1963) for upper-crustal *P* and *T*. This mode of K-enrichment in granites is more effective than could result from fluid-undersaturated partial melting of mica- and/or amphibole-bearing rocks. Conditioning of the mid-crust prior to anatexis by chloride brines could lead to the production of very K-rich granites.

4.2.3. *H_2O budget of anatexis*

Johannes and Holtz (1991) state, in their quantitative appraisal of granite magmas, that the amount of H_2O resident in hydrous minerals in possible source rocks would not be sufficient to account for major melt fractions at temperatures below about 900 °C. This limit to dehydration melting becomes even more stringent if the larger H_2O contents of the melts inferred from the present microprobe totals of quenched glasses are accepted. Migmatites showing large-volume melt segregation, the diatexites, are sometimes the products of transitional granulite-facies metamorphism. H_2O in some form at low activity must have been infiltrated into the site of anatexis.

Infiltration of a concentrated alkali-chloride brine would satisfy the condition of low H_2O activity while removing the restriction on the amount of H_2O that could be available for rock melting, so long as infiltration persists. Possible sources of saline fluids active in the deeper parts of the crust is a subject of considerable debate,

as outlined below. The infiltrating fluids, whatever their origin, would doubtless be channelized along deformation features, consonant with the frequent association of migmatite complexes and granite swarms with large-scale shear zones (Hutton, 1988; Liotta et al., 2004; Tikoff and Teyssier, 1992).

4.2.4. Mid-crustal migmatites

Several authors have called attention to the possibility that a mid-crustal migmatite layer several km thick may be characteristic of much of the continental interiors (Kruckenberg et al., 2008; Vanderhaeghe, 2009). Brown (2001) regarded this migmatite layer as the feeder zone for deep-crust-derived granite magmas that subsequently coalesced at upper crustal levels to form granite plutons. Others regard the migmatite layer as the source of the granites; escaping magmas have been arrested in situ by freezing (Johnson et al., 2003).

The concept of brine-assisted anatexis provides yet another hypothesis for a discrete mid-crustal migmatite zone. It is evident from Fig. 6 that rising aqueous fluids concentrated in alkali chlorides will, because of the positive dP/dT slopes of the brine-saturated minimum-melting isopleths, provoke melting at some threshold of decreasing pressure depending on the salt concentration of the fluids. For instance, a NaCl–KCl solution of $X_{H_2O} = 0.5$ generated or released at 800 °C and a depth equivalent to 10 kbar (about 35 km), and rising nearly isothermally (Harris et al., 1982), would traverse a quartzofeldspathic granulite-facies lower crust without producing major melting until a depth equivalent to ~7 kbar (~25 km) is reached, as shown in Fig. 6. For anatexis at incipient granulite grade, where orthopyroxene becomes stable relative to biotite, the P–T conditions may be about 5–7 kbar and 750–800 °C, according to the experimental work of Aranovich and Newton (1998). According to Fig. 6, these conditions are consistent with melting in the presence of a rising NaCl–KCl brine of $X_{H_2O} = 0.4$–0.6.

4.2.5. Ascent of fluid-saturated granitic magmas

The positive dP/dT slopes of the brine-saturated solidi would allow the ascent of fluid-saturated granitic magmas in the crust, once generated. The continual increase of H_2O activity with decreasing pressure of the saline fluids would allow further melting to occur in transit. The pressure interval below 3 kbar where the dP/dT slopes of all of the isopleths turn negative could possibly account for the high-level emplacement of granites. The accompanying salt solutions could then effect mineralization in the roof zones of the emplaced granite. It should be emphasized that, under this hypothesis, the salt solutions need not have been exsolved from the granite liquids, but may have merely accompanied them in ascent.

The ability of fluid-saturated granite magmas at any pressure to ascend would not be possible for pure H_2O pore fluids because the granite liquid would freeze at pressures less than those of the pure H_2O solidus at any temperature. Holloway (1976) suggested that CO_2-bearing pore fluids could allow ascending partially molten granites to exist, but, because of the high H_2O activities in CO_2 mixtures, it would take overwhelming concentrations of CO_2 in such fluids to lower H_2O activity sufficiently to turn the dP/dT slopes of H_2O isopleths positive, as shown in Fig. 6. Moreover, CO_2-rich fluids are quite inert in rock systems and would be unable to generate the metasomatism seen in some granites and migmatites, such as in the southern Closepet Granite area (Slaby et al., 2012).

Several possible sources have been suggested for concentrated brines which could be active in deep crustal metamorphism and anatexis. These include connate seawater or evaporates of marine origin (Yardley and Graham, 2002); concentration of dissolved salts in pore solutions by H_2O extracted into hydrous minerals during retrograde metamorphism (Markl and Bucher, 1998); downward circulation of brines of surficial origin in crustal-scale convection cells (Aranovich et al., 2010; McLelland et al., 2002); or degassing of crystallizing magmas at depth (Ryabchikov and Hamilton, 1971). The experiments of Webster et al. (2002) may be pertinent in this regard. They showed that, at pressures up to 2 kbar, Cl solubility in basalt magmas is many times greater than in granitic magmas at the same P and T. Therefore, if, as postulated by Litvinovsky and Podladchikov (1993), granitic magmas are commonly generated in the continental crust by melting in contact with volatile-rich, mantle-derived basalt intrusions, the Cl from the basalt would be discharged almost quantitatively and concentrated in saline fluids as H_2O is preferentially transmitted to the granitic magmas. Such a process may plausibly accompany basalt-triggered crustal melting in a range of settings (Hildreth, 1981). An example is continental extension in the Great Basin of the western USA, where there is high electrical conductivity of the deep crust in a region that has undergone bimodal mafic and felsic magmatism throughout the Tertiary and Quaternary Periods (Wannamaker et al., 2004). These authors postulate that the high electrical conductivity results from regionally interconnected saline pore solutions, and that these solutions emanate from the crystallization of basaltic intrusions at depth, providing a heat source, as well as a source of fluids.

5. Conclusions

(1) Concentrated (Na,K)Cl aqueous solutions raise the minimum melting temperature of haplogranite greatly relative to that for pure H_2O at pressures greater than about 3 kbar. The effect is much greater than for CO_2 solutions of the same H_2O concentrations and is due to the pressure-induced decrease of H_2O activity in the brines. The brine concentrations in question are in the range observed in fluid inclusions of some granites and migmatites.

(2) As a consequence, there exists a large P–T window in the deeper parts of the continental crust where salty solutions, which have been shown to be potent transport agents and reaction fluxes in rock systems, can effect subsolidus metasomatism at granulite facies conditions. These effects include dehydration, large-ion lithophile element depletion, and alkali exchange.

(3) First-melting isopleths at fixed X_{H_2O} in (Na,K)Cl solutions have strongly positive dP/dT slopes. Thus, salty solutions released into the deep crust may not provoke melting until they ascend to mid-crust levels. This provides an explanation for the characteristic mid-crust migmatite layer advocated by some workers.

(4) Unlike “dehydration melting” as a H_2O source for granitic magmas, there is no theoretical limit to the amount of H_2O available for melting, and therefore, the “fertility” of intermediate gneiss source rocks, even in the low-H_2O granulite facies, may be high, as long as brine infiltration persists.

(5) We have identified a “brine trend” of increasing K_2O concentration in haplogranite minimum melts with decreasing H_2O activity. This trend is similar to, but more pronounced than, the trend of granitic melts in the presence of CO_2–H_2O solutions, and may provide an explanation for the characteristic K-enrichment of A-type granites.

(6) Many sources of concentrated salt solutions have been proposed to explain the brine inclusions observed in minerals of some granites and migmatites. One of the most appealing is as degassing of crystallizing basaltic intrusions at depth, which could also be the principal heat source for metamorphism and anatexis.

Acknowledgments

The manuscript was improved by anonymous reviewers and the editorial advice of Tim Elliott. We gratefully acknowledge the help given by Frank Kyte in the microprobe analysis of the experimental run products. Mike Huh helped to prepare the probe mounts. Ben Newton made reconnaissance experiments to determine the appropriate ranges of run conditions. We thank Everett Shock for analyses of solutions for NaCl–KCl. Dirk Van Reenen gave much helpful discussion. The visit of L.Y. Aranovich to UCLA was made possible by a U.S. Fulbright Grant. The research was supported by the NSF EAR-1049901 (CEM).

Appendix A. Supplementary data

Supplementary data associated with this article can be found in the online version at http://dx.doi.org/10.1016/j.epsl.2013.05.027.

References

Anderson, J.L., Bender, E.E., 1989. Nature and origin of Proterozoic A-type granitic magmatism in the southwestern United States of America. Lithos 23, 19–52.
Antignano, A., Manning, C.E., 2008. Fluorapatite solubility in H_2O and H_2O–NaCl at 700 to 900 °C and 0.7 to 2.0 GPa. Chem. Geol. 251, 112–119.
Aranovich, L.Y., Bortnikov, N.S., Serebryakov, N.S., Sharkov, E.V., 2010. Conditions of the formation of plagiogranite from the Markov trough, Mid-Atlantic Ridge, 5°52′–6°02′N. Dokl. Earth Sci. 434, 1257–1262.
Aranovich, L.Y., Newton, R.C., 1996. H_2O activity in concentrated NaCl solutions at high pressures and temperatures measured by the brucite–periclase equilibrium. Contrib. Mineral. Petrol. 125, 200–212.
Aranovich, L.Y., Newton, R.C., 1997. H_2O activity in concentrated KCl and KCl–NaCl solutions at high temperatures and pressures measured by the brucite–periclase equilibrium. Contrib. Mineral. Petrol. 127, 261–271.
Aranovich, L.Y., Newton, R.C., 1998. Reversed determination of the reaction: phlogopite+quartz=enstatite+potassium feldspar+H_2O in the ranges 750–875 °C and 2–12 kbar at low H_2O activity with concentrated KCl solutions. Am. Mineral 83, 193–204.
Aranovich, L.Y., Newton, R.C., 1999. Experimental determination of CO_2–H_2O activity–composition relations at 600–1000 °C and 6–14 kbar by reversed decarbonation and dehydration reactions. Am. Mineral. 84, 1319–1332.
Berger, A., Burri, T., Alt-Epping, P., Engi, M., 2008. Tectonically controlled fluid flow and water-assisted melting in the middle crust: an example from the Central Alps. Lithos 102, 598–615.
Brown, M., 2001. Crustal melting and granite magmatism: key issues. Phys. Chem. Earth, Part. A: Solid Earth Geod. 26, 201–212.
Brown, W.L., Parsons, I., 1981. Towards a more practical two-feldspar geothermometer. Contrib. Mineral. Petrol. 76, 369–377.
Castro, A., Corretge, L.G., De la Rosa, J.D., Fernandez, C., Lopez, S., Garcia-Moreno, O., Chacon, H., 2003. The appinite–migmatite complex of Sanabria, NW Iberian massif, Spain. J. Petrol. 44, 1309–1344.
Cherneva, Z., Georgieva, M., 2007. Amphibole-bearing leucosome from the Chepelare area, Central Rhodopes: conditions of melting and crystallization. Geochem. Mineral. Petrol. 45, 79–95.
Devine, J.D., Gardner, J.E., Brack, H.P., Layne, G.D., Rutherford, M.J., 1995. Comparison of microanalytical methods for estimating H_2O contents of silicic volcanic glasses. Am. Mineral. 80, 319–328.
Ebadi, A., Johannes, W., 1991. Beginning of melting and composition of first melts in the system Qz–Ab–Or–H_2O–CO_2. Contrib. Mineral. Petrol. 106, 286–295.
Friend, C.R.L., 1983. The link between charnockite formation and granite production: evidence from Kabbaldurga, Karnataka, Southern India. In: Atherton, M.P., Gribble, D.C. (Eds.), Migmatites and Metamorphism. Shiva, Nantwich, pp. 264–276.
Goldsmith, J.R., Newton, R.C., 1974. An experimental determination of the alkali feldspar solvus. In: Mackenzie, W.S., Zussman, J. (Eds.), The Feldspars. Manchester University Press, Manchester, pp. 337–359.
Hansteen, T.H., Burke, E.A.J., 1990. Melt–mineral–fluid interaction in the Oslo Rift, southwest Norway. II. High temperature fluid inclusions in the Eikorn–Skrim complex. Nor. Geol. Unders. Bull. 417, 15–32.
Harris, C., 1986. A quantitative study of magmatic inclusions in the plutonic ejecta of Ascension Island. J. Petrol. 27, 251–276.
Harris, N.B.W., Holt, R.W., Drury, S.A., 1982. Geobarometry, geothermetry, and Late Archean geotherms from the granulite facies terrain of South India. J. Geol. 90, 509–527.
Harris, N.B.W., Marriner, G.F., 1980. Geochemistry and petrogenesis of a peralkaline granite complex from the Midian Mountains, Saudi Arabia. Lithos 13, 325–337.
Hildreth, W., 1981. Gradients in silicic magma chambers—implications for lithospheric magmatism. J. Geophys. Res. 86, 153–192.
Höller, W., Hoinkes, G., 1996. Fluid evolution during high-pressure partial melting in the Australalpine Ulten Zone, northern Italy. Mineral. Petrol. 58, 131–144.
Holloway, J.R., 1976. Fluids in the evolution of granitic magmas: consequences of finite CO_2 solubility. Geol. Soc. Am. Bull. 87, 1513–1518.
Holtz, F., Becker, A., Freise, M., Johannes, W., 2001. The water-undersaturated and dry Qz–Ab–Or system revisited. Experimental results at very low water activities and geological implications. Contrib. Mineral. Petrol. 141, 347–357.
Huang, W.-L., Wyllie, P.J., 1975. Melting reactions in the system $NaAlSi_3O_8$–$KAlSi_3O_8$–SiO_2 to 35 kilobars, dry and with excess water. J. Geol. 83, 737–748.
Hutton, D.H.W., 1988. Igneous emplacement in a shear-zone termination: the biotite granite of Strontian, Scotland. Geol. Soc. Am. Bull. 100, 1392–1399.
Iiyama, J.T., 1965. Influence des anions sur les équilibres d'échange d'ions Na-K dans les feldspaths alcalins a 600 °C sous une pression de 1000 bars. Bull. Soc. Fr. Minéral. Cristallogr. 88, 618–622.
Johannes, W., 1985a. The petrology of granite. Fortschr. Mineral. 63, 284.
Johannes, W., 1985b. The significance of experimental studies for the formation of migmatites. In: Ashworth, J.R. (Ed.), Migmatites. Blackie, Glasgow, pp. 36–85.
Johannes, W., Holtz, F., 1991. Formation and ascent of granitic magmas. Geol. Rundsch. 80, 225–231.
Johannes, W., Holtz, F., 1996. Petrogenesis and Experimental Petrology of Granitic Rocks. Springer, Berlin.
Johnson, T.E., Hudson, N.F.C., Droop, G.T.R., 2003. Evidence for a genetic granite–migmatite link in the Dalradian of NE Scotland. J. Geol. Soc. London 160, 447–457.
Jung, S., Hoernes, S., Masberg, P., Hoffer, E., 1999. The petrogenesis of some migmatites and granites (central Damara Orogen, Namibia): evidence for disequilibrium melting, wall–rock contamination and crystal fractionation. J. Petrol. 40, 1241–1269.
Kalsbeek, F., Jepsen, H.F., Jones, K.A., 2001. Geochemistry and petrogenesis of S-type granites in the East Greenland Caledonides. Lithos 57, 91–109.
Kerrick, D.M., Jacobs, G.K., 1981. A modified Redlich–Kwong equation for H_2O, CO_2, and H_2O–CO_2 mixtures at elevated pressures and temperatures. Am. J. Sci. 281, 735–767.
Kruckenberg, S.C., Whitney, D.L., Teyssier, C., Fanning, C.M., Dunlap, W.J., 2008. Paleocene–Eocene migmatite crystallization, extension, and exhumation in the hinterland of the northern Cordillera: Okanogan dome, Washington, USA. Geol. Soc. Am. Bull. 120, 912–929.
Liotta, D., Festa, J., Caggianelli, A., Prosser, G., Pascazio, A., 2004. Mid-crustal shear zone evolution in a syn-tectonic late Hercynian granitoid (Sila Massif, Calabria, southern Italy). Int. J. Earth Sci. 93, 400–413.
Lira, R., Poklepovic, M.F., Dorais, M.J., 2007. Solid inclusions of magmatic halite and sylvite in felsic granitoids, Sierra Norte, Cordoba, Argentina. Lithos 99, 363–384.
Litvinovsky, B.A., Podladchikov, Y.Y., 1993. Crustal anatexis during the influx of mantle volatiles. Lithos 30, 93–107.
Luth, W.C., Tuttle, O.F., Jahns, R.H., 1964. Granite system at pressure of 4 to 10 kilobars. J. Geophys. Res. 69, 759–773.
Markl, G., Bucher, K., 1998. Composition of fluids in the lower crust inferred from metamorphic salt in lower crustal rocks. Nature 391, 781–783.
McLelland, J., Morrison, J., Selleck, B., Cunningham, B., C., O., Schmidt, K., 2002. Hydrothermal alteration of late-to post-tectonic Lyon Mountain Granite Gneiss, Adirondack Mountains, New York: origin of quartz–sillimanite segregations, quartz–albite lithologies and associated Kiruna-type low-Ti oxide deposits. J. Metamorph. Geol. 20, 175–190.
Misiti, V., Tecce, F., Gaeta, M., 2005. Fluids in low-pressure migmatites: a fluid inclusion study of rocks from the Gennargentu Igneous Complex (Sardinia, Italy). Mineral. Petrol. 85, 253–268.
Newton, R.C., Manning, C.E., 2000. Quartz solubility in H_2O–NaCl and H_2O–CO_2 solutions at deep crust–upper mantle pressures and temperatures: 2–15 kbar and 500–900 °C. Geochim. Cosmochim. Acta 64, 1993–3005.
Newton, R.C., Manning, C.E., 2002. Experimental determination of calcite solubility in H_2O–NaCl solutions at deep crust/upper mantle pressures and temperatures: implications for metasomatic processes in shear zones. Am. Mineral. 87, 1401–1409.
Newton, R.C., Manning, C.E., 2006. Solubilities of corundum, wollastonite and quartz in H_2O–NaCl solutions at 800 °C and 10 kbar: interaction of simple minerals with brines at high pressure and temperature. Geochim. Cosmochim. Acta 70, 5571–5582.
Newton, R.C., Manning, C.E., 2007. Solubility of grossular, $Ca_3Al_2Si_3O_{12}$, in H_2O–NaCl solutions at 800 °C and 10 kbar, and the stability of garnet in the system $CaSiO_3$–Al_2O_3–H_2O–NaCl. Geochim. Cosmochim. Acta 71, 5191–5202.
Newton, R.C., Manning, C.E., 2008. Thermodynamics of SiO_2–H_2O fluid near the upper critical end point from quartz solubility measurements at 10 kbar. Earth Planet. Sci. Lett. 274, 241–249.
Newton, R.C., Manning, C.E., 2010. Role of saline fluids in deep-crustal and upper-mantle metasomatism: insights from experimental studies. Geofluids 10, 58–72.
Orville, P.M., 1963. Alkali ion exchange between vapor and feldspar phases. Am. J. Sci. 261, 201–237.
Parsons, I., 1978. Alkali-feldspars: which solvus? Phys. Chem. Miner. 2, 199–213.
Percival, J.A., 1991. Granulite-facies metamorphism and crustal magmatism in the Ashuanipi complex, Quebec-Labrador, Canada. J. Petrol. 32, 1261–1297.
Prince, C., Harris, N., Vance, D., 2001. Fluid-enhanced melting during prograde metamorphism. J. Geol. Soc. London 158, 233–241.
Roedder, E., 1971. Fluid inclusion studies on porphyry-type ore deposits at Bingham, Utah, Butte, Montana, and Climax, Colorado. Econ. Geol. 66, 98–120.

Rubatto, D., Hermann, J., Berger, A., Engi, M., 2009. Protracted fluid-induced melting during Barrovian metamorphism in the Central Alps. Contrib. Mineral. Petrol. 158, 703–722.
Ryabchikov, I.D., Hamilton, D.L., 1971. Possibility of concentrated chloride solutions in course of acid magma crystallization. Dokl. Akad. Nauk SSSR 197, 933–937.
Shen, A., Keppler, H., 1997. Direct observation of complete miscibility in the albite–H_2O system. Nature 385, 710–712.
Shmulovich, K., Graham, C., Yardley, B.W.D., 2001. Quartz, albite and diopside solubilities in H_2O–NaCl and H_2O–CO_2 fluids at 0.5–0.9 GPa. Contrib. Mineral. Petrol. 141, 95–108.
Slaby, E., Martin, H., Hamada, M., Smigielski, M., Domonik, A., Gotze, J., Hoefs, J., Halas, S., Simon, K., Devidal, J.L., Moyen, J.F., Jayananda, M., 2012. Evidence in Archaean alkali feldspar megacrysts for high-temperature interaction with mantle fluids. J. Petrol. 53, 67–98.
Slagstad, T., Jamieson, R.A., Culshaw, N.G., 2005. Formation, crystallization, and migration of melt in the mid-orogenic crust: Muskoka domain migmatites, Grenville Province, Ontario. J. Petrol. 46, 893–919.
Smit, C.A., Van Reenen, D.D., 1997. Deep crustal shear zones, high-grade tectonites, and associated metasomatic alteration in the Limpopo belt, South Africa: implications for deep crustal processes. J. Geol. 105, 37–57.
Srikantappa, C., Malathi, M.N., 2008. Solid inclusions of magmatic halite and CO_2–H_2O inclusions in the Closepet Granite from Ramnagaram, Dharwar Craton, India. Indian Mineral. 42, 84–89.
Srikantappa, C., Zargar, S.A., 2009. First report on the halite-bearing fluid inclusions in the Precambrian granulites around Halaguru, Dharwar Craton, India. Indian Mineral. 43, 77–80.
Stevens, G., Clemens, J.D., Droop, G.T.R., 1997. Melt production during granulite-facies anatexis: experimental data from "primitive" metasedimentary protoliths. Contrib. Mineral. Petrol. 128, 352–370.
Thompson, A.B., 2001. Clockwise P–T paths for crustal melting and H_2O recycling in granite source regions and migmatite terrains. Lithos 56, 33–45.
Tikoff, B., Teyssier, C., 1992. Crustal-scale, en echelon "P-shear" tensional bridges: a possible solution to the batholith room problem. Geology 20, 927–930.
Timmermann, H., Jamieson, R.A., Parrish, R.R., Culshaw, N.G., 2002. Coeval migmatites and granulites, Muskoka domain, southwestern Grenville Province, Ontario. Can. J. Earth Sci. 39, 239–258.
Touret, J., Olsen, S.N., 1985. Fluid inclusions in migmatites. In: Ashworth, J.R. (Ed.), Migmatites. Chapman and Hall, New York, pp. 265–286.
Tropper, P., Manning, C., Harlov, D., 2011. Solubility of $CePO_4$ monazite and YPO_4 xenotime in H_2O and H_2O–NaCl at 800 °C and 1 GPa: implications for REE and Y transport during high-grade metamorphism. Chem. Geol. 282, 58–66.
Tuttle, O.F., Bowen, N.L., 1958. Origin of granite in the light of experimental studies in the system $NaAlSi_3O_8$–$KAlSi_3O_8$–SiO_2–H_2O. Geol. Soc. Am. Mem. 74, 1–153.
Vanderhaeghe, O., 2009. Migmatites, granites and orogeny: flow modes of partially-molten rocks and magmas associated with melt/solid segregation in orogenic belts. Tectonophysics 477, 119–134.
Wannamaker, P.E., Caldwell, T.G., Doerner, W.M., Jiracek, G.R., 2004. Fault zone fluids and seismicity in compressional environments inferred from electrical conductivity: the New Zealand southern Alps and US Great Basin. Earth, Planets Space 56, 1171–1176.
Webster, J.D., Kinzler, R.J., Mathez, E.A., 2002. Chloride and water solubility in basalt and andesite liquids and implications for magmatic degassing. Geochim. Cosmochim. Acta 63, 729–738.
Yardley, B.W.D., Graham, J.T., 2002. The origins of salinity in metamorphic fluids. Geofluids 2, 249–256.
Yund, R.A., Tullis, J., 1983. Subsolidus phase relations in the alkali feldspars with emphasis on coherent phases. Rev. Mineral. 2, 141–176.